Chemical Engineering Journal 154 (2009) 60–68

Contents lists available at ScienceDirect

Chemical Engineering Journal

journal homepage: www.elsevier.com/locate/cej

Oxidation of β-picoline to nicotinic acid over V_2O_5-TiO_2 catalyst: Kinetic studies and reaction mechanism

E.V. Ovchinnikova*, T.V. Andrushkevich, G.Ya. Popova, V.D. Meshcheryakov, V.A. Chumachenko

Boreskov Institute of Catalysis SB RAS (BIC), Postal address: Pr. Akademika Lavrentieva 5, Novosibirsk 630090, Russia

ARTICLE INFO

Article history:
Received 30 December 2008
Received in revised form 19 March 2009
Accepted 8 April 2009

Keywords:
β-Picoline
Kinetic model
Nicotinic acid
Vanadia-titania catalyst

ABSTRACT

Kinetic model of β-picoline oxidation to nicotinic acid over V_2O_5-TiO_2 catalyst in the temperature range 270–300 °C was elaborated on the base of the experimental data obtained in a differential reactor. Reaction mechanism was studied by *in situ* FTIR method. Kinetic parameters of the reaction rates were evaluated. The model gives satisfactory agreement between predicted and experimental results over a wide range of experimental conditions.

1. Introduction

Vanadium-titanium catalysts are widely used in many processes of selective oxidation of hydrocarbons [1–4]. For example, V_2O_5-TiO_2 or V-containing catalysts were intensively studied in oxidation and ammoxidation of aromatic compounds [2–5], in particular of toluene [6–10] and *o*-xylene [1,9,11–16], picolines [5,17–29]. V_2O_5-TiO_2 catalysts show high selectivity in gas-phase oxidation of β-picoline to nicotinic acid [25–28].

Nicotinic acid (niacin, NA) is a valuable chemical product and an important vitamin of B group. Specific action of this vitamin consists in prevention and treatment of pellagra disease. Niacin is widely used in medicine, in food industry, in agriculture, in production of cosmetics [30]. Annual worldwide output of nicotinic acid is ~34,000 ton ('2000 estimate).

Nicotinic acid is produced commercially by oxidation of 2-methyl-5-ethylpyridine or 3-methylpyridine (β-picoline, βP) in liquid phase or in gas phase. Processes of liquid-phase oxidation by potassium permanganate, or nitric acid, or sulfuric acid are performed at high pressure [31]. Nicotinic acid is formed via hydrolysis of pyridine-3-nitrile that is produced by ammoxidation of (P in the presence of vanadia catalyst [32–34]. The use βP as feedstock is commercially reasonable, because the price of 2-methyl-5-ethylpyridine is on average 2 times higher than that of βP and approaches to the price for nicotinic acid.

Boreskov Institute of Catalysis (BIC) has developed a direct one-step method of nicotinic acid synthesis by gas-phase oxidation of β-picoline by air over proprietary vanadia-titania catalyst [25]. The process produces no liquid wastes and no harmful gas exhausts, and the target product can be easily extracted. In total, the process meets all requirements of "green" technology [30,35,36].

For proper practical implementation of NA process, an adequate kinetic model of reactions based upon detailed reaction mechanism is required.

In the literature, there is a lack of research on the mechanism and kinetics of β-picoline oxidation over V_2O_5-TiO_2 catalyst [26,37,38], as well as on oxidation over CrVPO [39,40] and CrAlVO [41] catalysts.

Surface compounds of adsorbed 3-picoline [37,40], pyridine-3-carbaldehyde [38], and pyridine-3-nitrile [42] were determined by *in situ* DRIFTS [40] and FTIR [37,38,42] at temperatures of β-picoline oxidation. Conversion of β-picoline proceeds through sequential turns into aldehyde-like intermediates and then into carboxylates which are direct precursors of NA. Redox mechanism of the product formation that was suggested in oxidation of picolines over CrVPO [39,40] catalyst can be accepted for V_2O_5-TiO_2 catalyst [36] as well. Associative mechanism of nicotinic acid formation was suggested in oxidation of βP over V_2O_5-TiO_2 catalyst [37,38].

Oxidation of picolines may be represented as parallel-consecutive network via formation of aldehyde as intermediate and assuming deep oxidation of picolines and products [26,28,29,39,40]. In the kinetic rate-controlled area, consecutive route of NA formation through intermediate PA prevails [26]. In diffusion-controlled area over commercial catalyst particles 4 mm × 2 mm × 5 mm (OD × ID × L), NA can be formed directly from βP [43] via parallel route.

This research concentrates on experimental study of the reaction mechanism and reaction rates of βP oxidation over vanadia-titania

---

* Corresponding author. Tel.: +7 383 3269412.
E-mail address: evo@catalysis.ru (E.V. Ovchinnikova).

1385-8947/$ – see front matter © 2009 Elsevier B.V. All rights reserved.
doi:10.1016/j.cej.2009.04.034

catalyst. We developed a kinetic model and estimated the parameters of kinetic equations.

2. Experimental

2.1. Catalyst

Catalyst (20%V_2O_5 + 80%TiO_2, %wt.) was prepared by spray drying of a mixture of titanium dioxide and solution of vanadyl oxalate [25]. Titanium dioxide of anatase modification prepared according to sulfate technology was used. Ring-shaped particles of 4 mm diameter, 5 mm length, and 1 mm wall thickness were prepared from the spray drying powder and then were calcinated at 450 °C in air flow. The BET specific surface area of the catalyst (S_{CAT}) was 25 $m^2\,g^{-1}$. According to XRD data, the catalyst contained phases of V_2O_5 and TiO_2 in anatase form. Method of differential dissolution was used for analysis of phase composition [44]. Catalyst contained ~40% of vanadium as V_2O_5 phase, while the rest of ~60%—as monolayer $[VO_X]_n$ species [45].

2.2. Scheme of the experimental set-up

Stationary activity of the catalyst was tested in a differential reactor of a flow-circulating set-up (see Fig. 1). A glass 15 mm reactor (OD) was equipped with 5 mm coaxial thermocouple pocket. Temperature in circulating loop was maintained at 130 °C, flow rate was 1.5–20 l h^{-1}, and circulating flow was 700–1000 l h^{-1}.

Flows of gaseous reactants were stabilized by flow-mass controllers; βP and water were dosed separately by saturating of nitrogen streams, followed by their condensation at preset temperature in reverse cooler.

2.3. Analysis of components

GC analysis of βP and of the reaction products was employed using TC detector. The inlet βP and CO_2 were analyzed in gas phase over Porapak-Q (length of column—2000 mm, ID—3 mm); O_2, N_2 and CO—over molecular sieves CaA (length of column—2000 mm, ID—3 mm). Unreacted βP and products of partial oxidation, such as pyridine-3-carbaldehyde (PA), pyridine-3-nitrile (PN) and pyridine (Py), were trapped at −78 °C and then analyzed in liquid phase over Chromosorb (length of column—3000 mm, ID—2 mm) using FI detector. No traces of HCN were observed.

The quantity of NA was calculated as the difference between the amount of converted βP and the amount of reaction products, assuming 100% balance. This assumption was verified experimentally by picking-up crystallized nicotinic acid just after the reactor outlet.

2.4. Reaction conditions

The contact time was varied by changing either the weight of the catalyst, or the flow rate of the gaseous mixture. The gas hourly space velocity (GHSV) was within 700–14,000 h^{-1}. The free space of the reactor was filled with quartz chips. The experiments were carried out at temperatures of 270–300 °C. The composition of inlet reaction mixture was (mol.%): βP 0.1–0.8, O_2 8–23, H_2O 5–25, and nitrogen balance. The concentration of nicotinic acid measured by its vapor pressure at 130 °C (at the temperature of the thermostat), that is, at the temperature of the circuit thermostat, was equal to 0.16 mol.% in all experiments.

The rates of products accumulation and selectivities were calculated with respect to the converted βP, taking into account stoichiometric coefficients of the individual reactions.

2.5. Formulas for calculation

Degree of βP conversion:

$$X = \frac{C^0_{\beta P} - C_{\beta P}}{C^0_{\beta P}} \times 100\%;$$

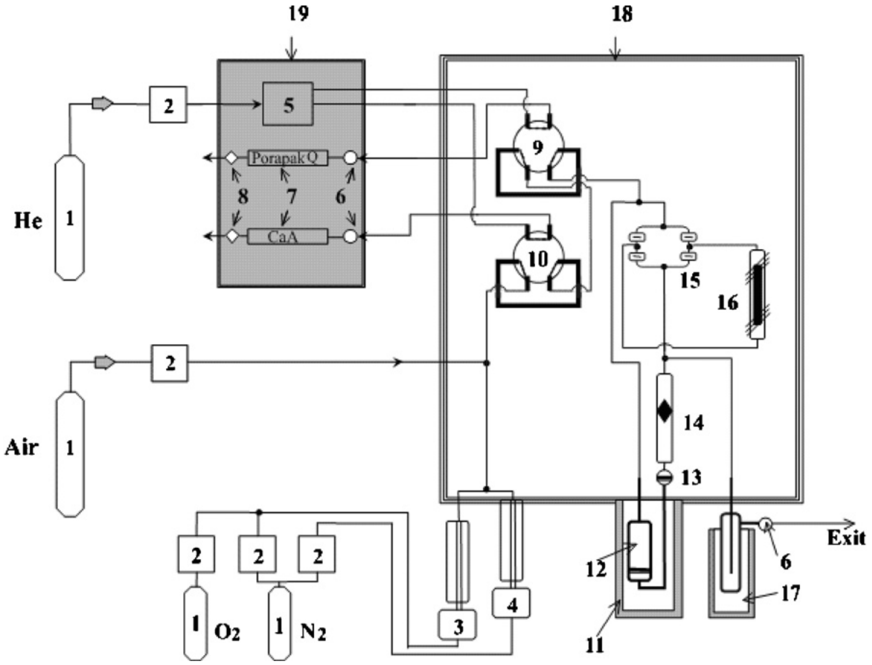

Fig. 1. The scheme of a lab set-up. 1—gas cylinders; 2—flow-mass controllers; 3—H_2O vaporizer; 4—βP vaporizer; 5—distributor; 6—sampling devices; 7—GC column; 8—detector; 9, 10—six-way valves; 11—furnace filled with fluidized sand; 12—reactor; 13—filter; 14—rotameter; 15—valve unit; 16—electromagnetic pump; 17—refrigerator; 18, 19—thermostat.

Rate of βP consumption:

$$W_{\beta P} = (C^0_{\beta P} - C_{\beta P}) \cdot \frac{V_f}{360 \cdot G \cdot S_{CAT} \cdot 22.4}, \ \mathrm{mol\,m^{-2}\,s^{-1}};$$

Rates of accumulation of PA, PN, CO_X:

$$W_i = \frac{C_i}{\nu_i} \cdot \frac{V_f}{360 \cdot G \cdot S_{CAT} \cdot 22.4}, \ \mathrm{mol\,m^{-2}\,s^{-1}};$$

Selectivities to PA, PN, CO_X:

$$S_i = \frac{W_i}{\nu_i \cdot W_{\beta P}} \times 100\%;$$

Contact time:

$$\tau = \frac{G \cdot 3600}{V_f \cdot \gamma};$$

where $C^0_{\beta P}$ is the inlet concentration of βP; $C_{\beta P}$ is the outlet concentration of βP; C_i is the outlet concentration of *i*th product, *i* = 1, 2, 3 respectively, for PA, PN, CO_X, mol.%; τ is the contact time, s; V_f is the flow rate at standard conditions, $m^3\,h^{-1}$; *G* is the weight of sample, g; S_{CAT} is the specific surface area, $m^2\,g^{-1}$; γ is the bulk density of catalyst, 0.85 g cm^{-3}; ν is the stoichiometric coefficient, $\nu = 1$ for βP, PA, NA and PN, $\nu = 6$ for CO_X.

3. Results and discussion

3.1. The general network of βP oxidation

Oxidation of β-picoline over V-Ti-O catalyst results in formation of nicotinic acid, pyridine-3-carbaldehyde, pyridine-3-nitrile, pyridine, CO_2 and CO as reaction products.

Kinetic reaction rates of (P transformation were studied at inlet composition βP:O_2:H_2O = 1.1:22:20 (mol.%), N_2 as balance, concentration of NA being invariable. Experiments were performed at 270, 285, and 300 °C in the range of *X* = 20–92%. Contact time was varied by means of changing either the weight of the catalyst or flow rate.

Reaction selectivity to products and the rates of the products formation depending on βP conversion are shown in Fig. 2. For all conversion values NA was the main reaction product, while selectivities to pyridine and CO were less than 0.5% (S_{Py} is not shown in Fig. 2).

Extrapolating selectivities to a zero conversion, one can reveal how parallel stages contribute to the reaction. It is possible to estimate with sufficient reliability only the contribution of parallel routes to CO_X (CO + CO_2) and PN formation as by-products. At 270 °C, the total of initial selectivities to CO_X and to PN does not exceed 3%, and tends to grow with the temperature. Monotonous increase in selectivity to CO_X with increase in βP conversion can be attributed to subsequent oxidation of the target products. Additional studies of individual NA oxidation in the same temperature range confirmed that NA can be converted into PN and CO_X [46].

Variation of selectivity to NA and PA with βP conversion indicates that the definite fraction of NA forms under the consecutive route through PA as an intermediate. The extrapolation of NA and PA selectivities to zero conversion

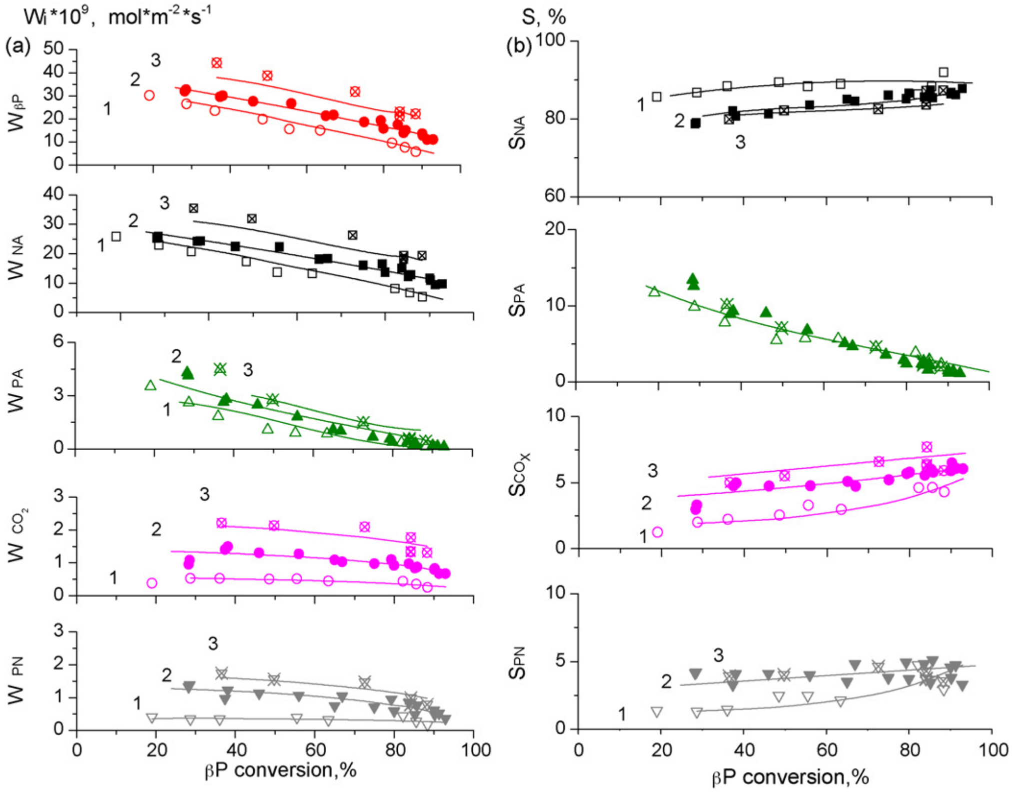

Fig. 2. Rates of the reactants accumulation (a) and selectivities to the products (b) vs. β-picoline conversion at 270 °C (1), 285 °C (2) and 300 °C (3). Lines are calculated values, points are experimental values.
GHSV = 910–20,000 h^{-1}; inlet gas composition βP:O_2: H_2O = 1:22:20 (mol.%).

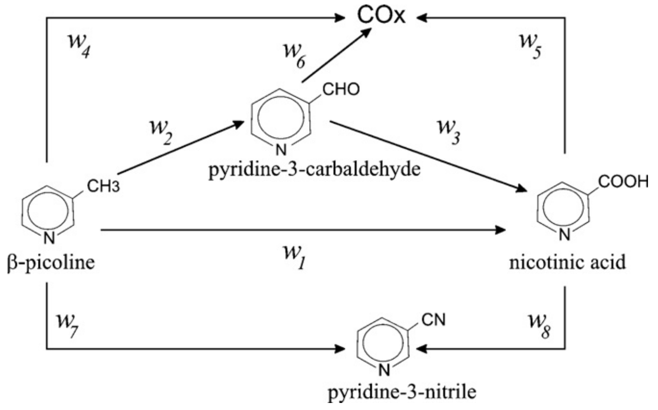

Scheme 1. Network of reaction products formed during β-picoline oxidation over a V-Ti catalyst. Here w_j are the product formation rates (j = 1–8): 1 *and* 3 denote the NA formation from βP and PA; 2 is the PA formation from βP; 4, 5, *and* 6 denote the CO_X formation from βP, NA and PA, respectively; 7 *and* 8 are the PN formation from βP and NA.

can provide a rough estimate of contribution of parallel routes.

Apparent reaction rates of these routes were calculated for catalyst particles 4 mm × 2 mm × 5 mm (OD × ID × L), basing on experimental data obtained in kinetic control region and considering diffusion limitations [47]. The general parallel-consecutive network of products formation in βP oxidation is shown in Scheme 1.

The following balance Eqs. (1)–(5) for accumulation rates of nicotinic acid (W_{NA}), pyridine-3-carbaldehyde (W_{PA}), carbon oxides (W_{CO_X}), pyridine-3-nitrile (W_{PN}) and the consumption rate of β-picoline ($W_{\beta P}$) can be written:

$$-W_{\beta P} = w_1 + w_2 + w_4 + w_7; \qquad (1)$$

$$W_{NA} = w_1 + w_3 - w_5 - w_8; \qquad (2)$$

$$W_{PA} = w_2 - w_3 - w_6; \qquad (3)$$

$$W_{CO_X} = w_4 + w_5 + w_6; \qquad (4)$$

$$W_{PN} = w_7 + w_8. \qquad (5)$$

Here w_j are rates of jth route (j = 1, 2, . . ., 8).

3.2. Role of individual components of reaction mixture

Experiments were carried out at temperature 270 °C in monoparametric mode, i.e., by varying only one parameter of the study, the other being unchanged.

The effect of β-picoline was studied at conversion of βP $X = 60 \pm 2\%$, concentrations of oxygen, water vapor and NA being fixed. Inlet concentration of β-picoline was varied in the range from 0.3 to 1.0 mol.%. The inlet reaction mixture contained O_2:H_2O (mol.%) = 22:20, the rest was nitrogen. Fig. 3 shows how reaction rates and selectivities of products were influenced by the actual concentration of βP.

The concentration of βP has significant influence on β-picoline conversion, on product accumulation and on selectivities. The rates of β-picoline conversion, NA, PA and PN accumulation in the range of 0.2–0.5 mol.% βP are described by the curves with saturation (Fig. 3a). The rates of CO_X formation (Fig. 3a) slightly vary within the entire range of β-picoline concentrations.

Selectivities to NA and PA were observed to change in the opposite ways (Fig. 3b). An increase in selectivity to PA is accompanied by a decrease in selectivity to NA. This can be attributed to a decrease in the rate of NA formation via consecutive route with an increase in the concentration of β-picoline. Only minor variations of selectivities to PN, CO_X (Fig. 3b) with variation of βP were revealed.

The effect of oxygen was studied at fixed concentration of β-picoline, water vapor (20 mol.%) and nicotinic acid (0.16 mol.%), and at $X = 60 \pm 1\%$. Concentration of β-picoline in the inlet reaction mixture was kept within 1.00 ± 0.05 mol.%. The oxygen concentration in the inlet reaction mixture was changed from 10 to 25 mol.%.

A high concentration ratio of oxygen to oxidizable reagent is typical in the selective oxidation of heterocyclic compounds [2,28,39–41,48], including β-picoline [18,27,39–41].

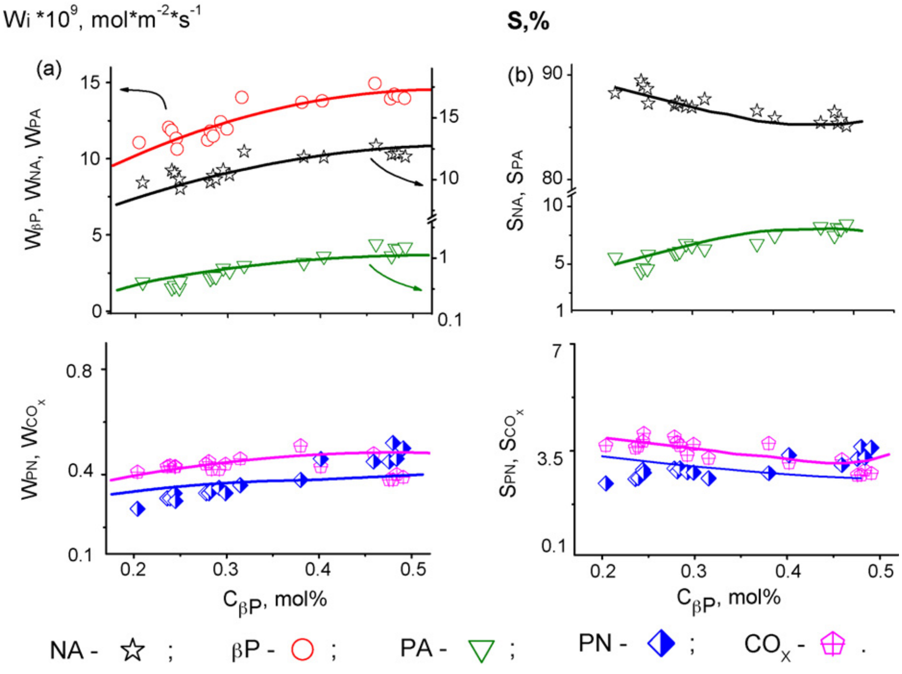

Fig. 3. Rates of the reactants accumulation (a) and selectivity to the products (b) vs. steady-state concentration of β-picoline. Lines are calculated (a) or fitting (b) values, points are experimental values. $X = 60 \pm 1\%$; $T = 270$ °C; GHSV = 3400–5300 h^{-1}; inlet gas composition βP:O_2:H_2O = (0.33–1.1):22:20 (mol.%).

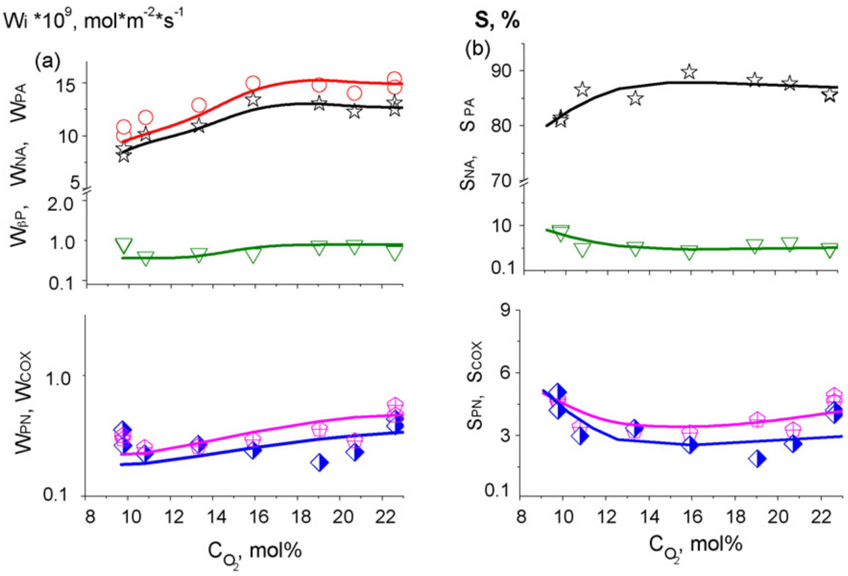

Fig. 4. Rates of the reactants accumulation (a) and selectivity to the products (b) vs. steady-state concentration of oxygen. Lines are calculated (a) or fitting (b) values, points are experimental values. Nomenclature of symbols see Fig. 3. $X = 60 \pm 1\%$; $T = 270\,^{\circ}C$; GHSV = 3050–4050 h^{-1}; βP:O_2:H_2O = 1:(9–23):20 (mol.%).

Fig. 4 shows how reaction rates and selectivities of products are influenced by the actual concentration of oxygen. Concentration of oxygen has different effects on the rates of specific reactions.

The rate of βP consumption and the rate of NA accumulation (Fig. 4a) reveal a tendency to saturation as oxygen concentration increases. The curves are coming to a plateau at C_{O_2} above 16 mol.%.

As to PA, PN, CO_X, the rates of accumulation remain just constant over the entire range of oxygen concentrations (Fig. 4a).

The selectivity to NA increases with a rise of C_{O_2} (Fig. 4b). Selectivities to PA, PN and CO_X are high at 9–12 mol.% oxygen, then decline and slightly grow at higher concentrations of oxygen. High selectivity to PN and CO_X at low concentration of the oxygen can be explained by partial reduction of the catalyst.

The influence of water vapor was studied at a fixed degree of βP conversion. Inlet reaction mixture contained (mol.%): βP—1, oxygen—18, steam was varied from 5 to 25, nitrogen balanced. Taking into account the parallel-consecutive network of the products formation, we carried out tests at conversions of β-picoline ~30% and at ~80%. At low conversion, the effect of water on the parallel stages can be cleared, whereas at high conversion, the effect of water on the consecutive stages can be cleared. The positive influence of water in selective oxidation of hydrocarbons was known earlier [49,50]. As to acids' formation, it is commonly adopted that water promotes desorption of the acid [51–53]. Also, water can modify the structure or acidity of active sites of vanadia-titania catalyst, which accelerates formation of products or intermediates [54].

Table 1a demonstrates changes in the rates of βP consumption and product accumulation and selectivities depending on water concentration.

As it is seen from the Table 1a, at 30% βP conversion the rate of βP transformation $W_{βP}$ is greatly influenced by water. This effect is displayed at the stages of W_{NA} and W_{PA} formation, as well as at the stage of PA oxidation to NA. Increase in the rate of accumulation of PA and decrease in its selectivity was observed under increasing water concentration. Water has a slight effect on the production of PN and CO_X. Water causes primarily the increase in selectivity to NA and PA and decrease in selectivity to PN and CO_X. Small increase in the rate of CO_X formation correlates to an increase in the rate of NA accumulation.

Reaction rates and selectivities to products at the degree of high βP conversion depend on water concentration as shown in Table 1b. There is no strong influence of water in this area, only slight change in the rates was observed, while selectivities remain constant in the whole interval of water concentration.

From this evidence it can be concluded that water does not affect further oxidation of nicotinic acid as well as further oxidation of other partial products. This observation was confirmed by a special

Table 1
Effect of water. Inlet gas composition βP:O_2:H_2O = 1:18:(5–25) (mol.%); $T = 270\,^{\circ}C$, GHSV = 1700–13,900 h^{-1}.

X (%)	C_{H_2O} (vol.%)	$W \times 10^{-9}$ (mol m^{-2} s^{-1})					S (%)				$V_f \times 10^{-3}$ (m^3 h^{-1})	G (g)
		βP	Na	CO_X	PA	PN	Na	CO_X	PA	PN		
a												
30	25	28.5	24.3	0.53	3.23	0.51	85.0	1.8	11.4	1.8	13.5	0.8
29	20	26.3	22.4	0.52	2.99	0.45	85.0	2.0	11.4	1.7	13.5	0.8
30	15	15.3	12.2	0.42	2.29	0.40	79.7	2.7	14.9	2.6	13.3	1.5
30	10	12.4	9.8	0.38	1.84	0.33	79.3	3.1	14.9	2.7	13.3	1.8
30	5	11.4	8.9	0.35	1.86	0.31	78.0	3.1	16.3	2.7	13.5	2.0
b												
79	25	9.6	8.3	0.44	0.36	0.43	87.2	4.6	3.7	4.5	20.2	9.0
81	20	9.4	8.2	0.46	0.33	0.42	87.0	4.9	3.5	4.5	20.0	9.0
80	15	9.4	8.2	0.44	0.34	0.40	87.4	4.7	3.6	4.3	20.0	9.0
80	10	9.0	7.9	0.41	0.32	0.41	87.3	4.6	3.6	4.5	19.8	9.0
80	5	8.7	7.5	0.38	0.36	0.42	86.8	4.4	4.1	4.8	18.3	9.0

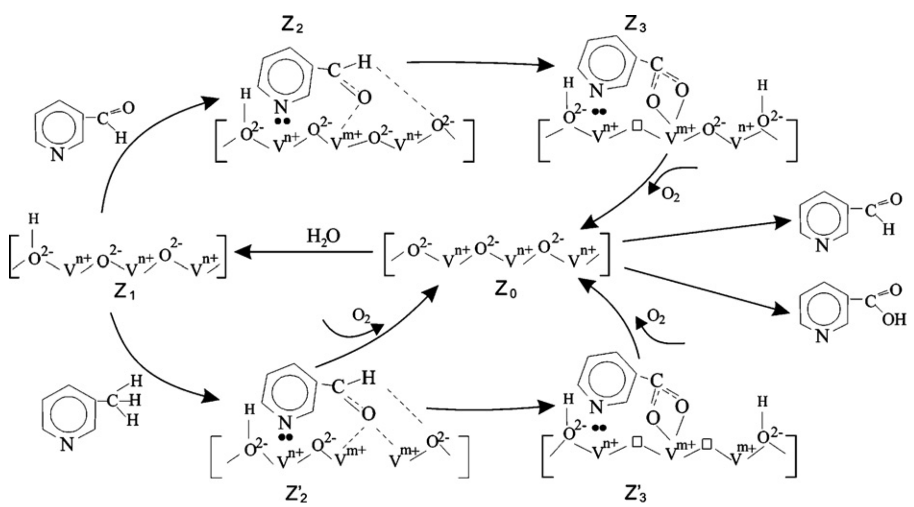

Scheme 2. Surface complexes of β-picoline and pyridine-3-carbaldehyde. Here Z_0 is an oxidized site, Z_1 is a hydrated site, Z_2 and Z'_2 are carbonyl complexes, Z_3 and Z'_3 are carboxylate complexes.

study of direct oxidation of NA [46]. We suppose that modification of structure or acidity of active sites could enhance the rates of stages that lead to NA and PA formation. The latter was shown for a vanadia-titania catalyst of the composition close to ours [54].

3.3. *Kinetic model*

Surface complexes of adsorbed (P and PA were identified using FTIR *in situ* method [37,38], and the mechanism of their transformation to NA was exhibited, as shown in Scheme 2. A kinetic model was constructed on the base of (i) comprehensive study of the reaction rates, (ii) the scheme of reactions, and (iii) the detailed mechanism of NA formation. The fundamental backgrounds of the kinetic model are the following.

- Investigation of the surface compounds showed that in the course of adsorption of both β-picoline [37] and PA [38] nicotinic acid forms through a sequence of similar surface complexes over active sites $[Z_0]$, like as $[VO_X]_n$.
- Experimentally observed dependence of βP conversion rate (as well as PA and NA formation rates) on concentration of water proved that selective oxidation proceeds over hydrated active sites $[VO_X]_n{\cdot}H_2O$ denoted as $[Z_1]$ hydroxyl groups over site $[Z_1]$ are not shown in Scheme 2).
- As a result of βP or PA adsorption, the surface complexes $[Z_2]$ and $[Z'_2]$ have an aldehyde-like structure. They transform into carboxyl complexes $[Z'_3]$ or $[Z_3]$ with different numbers of oxygen atoms. These carboxyl complexes are the immediate precursors of nicotinic acid.
- When studying PA adsorption, we observed the complex $[Z_2]$ at temperatures below the reaction temperature. It quickly transforms to the complex $[Z_3]$. Therefore, we did not take into account these fast steps while constructing the kinetic model.
- An oxygen atom of the catalyst participates in the formation of surface complexes $[Z'_2]$, $[Z'_3]$ and $[Z_3]$. Taking into account high mobility of bulk oxygen in V-Ti catalyst that makes the surface oxygen homogeneous in a wide range of coverage, we assumed that the oxygen atoms in these complexes are equivalent, adsorption energy to be 230–250 kJ mol^{-1} [55].
- Transformation of complex $[Z'_2]$ into aldehyde and transformation of complexes $[Z'_3]$ and $[Z_3]$ into acid occurs with the participation of molecular oxygen in a stage that is joined with the stage of catalyst reoxidation [56]. Similar influence of oxygen was first time observed in oxidation of *o*-xylene [11]. Later, the same mechanism was revealed in oxidation of formaldehyde to formic acid [57].
- No surface complexes that could act as intermediates in deep oxidation to CO_X were distinguished by FTIR spectroscopy, most likely, due to a low activity of V_2O_5-TiO_2 catalyst in such reactions. Basing upon the current data [58] and our previous studies [59–60], we assumed that strongly bound carbonate–carboxylate complexes are the surface compounds that can act as said intermediates. These complexes can be oxidized by gaseous or weakly bound oxygen [61]. Deep oxidation of βP, PA and NA occurs on active sites named $[Z''_0]$, while selective oxidation proceeds on other sites $[Z_0]$.
- A complex titled $[Z_N]$ interacts with βP and NA, thus resulting to PN formation at the sites. FTIR spectroscopy study revealed surface complexes of $NH_4{}^+$. These complexes form when NA, PA, βP oxidize to CO_X at the temperatures of the reaction [42]. This mechanism is confirmed by experimental facts, namely (i) selectivity to PN and CO_X are similar in a wide range of βP conversion (Fig. 1), and (ii) rate of PN formation depends on concentration of oxygen [62].

Proceeding on these assumptions, one can express the reaction scheme by stages as follows (here r_m is the rate of mth stage, $m = 1, 2, \ldots, 17$).

3.3.1. *Formation of nicotinic acid and pyridine-3-carbaldehyde (stages 1–7):*

1. $Z_0 + H_2O \xrightarrow{r_1} Z_1$;
2. $Z_1 + \beta P \xrightarrow{r_2} Z'_2$;
3. $Z'_2 + O_2 \xrightarrow{r_3} Z_0 + H_2O + PA$;
4. $Z'_2 \xrightarrow{r_4} Z'_3$;
5. $Z'_3 + O_2 \xrightarrow{r_5} Z_0 + H_2O + NA$;
6. $Z_1 + PA \xrightarrow{r_6} Z_3$;
7. $Z_3 + O_2 \xrightarrow{r_7} Z_0 + H_2O + NA$;

See notations to Scheme 2.

3.3.2. *Formation of CO_2 from βP, PA and NA (stages 8–13):*

8. $Z''_0 + \beta P \xrightarrow{r_8} Z''_1$;
9. $Z''_1 + O_2 \xrightarrow{O_2,\, r_9} Z''_0 + H_2O + CO_2$;
10. $Z''_0 + PA \xrightarrow{r_{10}} Z''_2$;
11. $Z''_2 + O_2 \xrightarrow{O_2,\, r_{11}} Z''_0 + H_2O + CO_2$;

Table 2
Kinetic parameters of β-picoline oxidation over V_2O_5-TiO_2 catalyst at 270 °C.

Rate equation	Constant	Dimension	$\mu \pm \sqrt{\sigma^2}/2$	E (kJ mol^{-1})
NA formation from βP: $w_1 = \frac{K_1 \cdot C_{\beta P}}{DEN1}$	K_1	s^{-1}	3.950 ± 0.089	44.0
PA formation from βP: $w_2 = \frac{K_1 \cdot K_3 \cdot C_{\beta P} \cdot C_{O_2}}{DEN1}$	K_2	s^{-1}	2.940 ± 0.117	42.3
NA formation from PA: $w_3 = \frac{K_2 \cdot C_{PA} \cdot (1+K_3 \cdot C_{O_2})}{DEN1}$	K_3	$m^3\ mol^{-1}$	0.0203 ± 0.002	1.7
CO_X formation from βP: $w_4 = \frac{K_4 \cdot C_{\beta P}}{DEN2}$	K_4	s^{-1}	0.4670 ± 0.026	24.3
CO_X formation from PA: $w_5 = \frac{K_5 \cdot C_{NA}}{DEN2}$	K_5	s^{-1}	0.1931 ± 0.004	37.3
CO_X formation from NA: $w_6 = \frac{K_6 \cdot C_{PA}}{DEN2}$	K_6	s^{-1}	0.1374 ± 0.004	25.1
PN formation from βP: $w_7 = \frac{K_7 \cdot C_{\beta P}}{DEN3}$	K_7	s^{-1}	0.4241 ± 0.016	31.0
PN formation from NA: $w_8 = \frac{K_8 \cdot C_{NA}}{DEN3}$	K_8	s^{-1}	0.2262 ± 0.01	26.4
$DEN1 = 1 + K_1 \cdot C_{\beta P} \cdot \left(K_{11} + \frac{K_{12}}{C_{O_2}} + \frac{K_9}{C_{H_2O}} + \frac{K_9 \cdot K_3 \cdot C_{O_2}}{C_{H_2O}}\right) + K_2 \cdot C_{PA} \cdot \left(K_3 \cdot K_{10} + \frac{K_{10}}{C_{O_2}} + \frac{K_9}{C_{H_2O}} + \frac{K_9 \cdot K_3 \cdot C_{O_2}}{C_{H_2O}}\right) + K_3 \cdot C_{O_2}$;	K_9	s	2.06 ± 0.117	7.5
	K_{10}	s	121 ± 2.45	−3.4
	K_{11}	$s\ m^3\ mol^{-1}$	0.19 ± 0.024	−26.4
	K_{12}	s	6 ± 0.332	−3.3
$DEN2 = 1 + \frac{K_{13} \cdot C_{\beta P}}{C_{O_2}} + \frac{K_{14} \cdot C_{NA}}{C_{O_2}} + \frac{K_{15} \cdot C_{PA}}{C_{O_2}}$;	K_{13}	–	294 ± 1	0
	K_{14}	–	349 ± 1	0
$DEN3 = 1 + \frac{K_{16} \cdot C_{\beta P}}{C_{O_2}} + \frac{K_{17} \cdot C_{NA}}{C_{O_2}}$	K_{15}	–	299 ± 1	0
	K_{16}	–	379 ± 10.3	2.1
	K_{17}	–	314 ± 7.06	8.8

Here C_{O_2}, C_{H_2O}, C_{NA}, and C_{PA} are the steady-state concentrations of the reaction mixture components βP, O_2, H_2O, PA, NA, respectively, mol m^{-3}; K_i are the parameters of the kinetic equations; E_i are apparent energy activations; k_m are the rate constants of stages. $K_1 = k_2$; $K_2 = k_6$; $K_4 = k_8$; $K_5 = k_{12}$; $K_6 = k_{10}$; $K_7 = k_{14}$; $K_8 = k_{16}$; $K_3 = k_3/k_4$; $K_9 = 1/k_1$; $K_{10} = 1/k_7$; $K_{11} = 1/k_4$; $K_{12} = 1/k_5$; $K_{13} = k_8/k_9$; $K_{14} = k_{12}/k_{13}$; $K_{15} = k_{10}/k_{11}$; $K_{16} = k_{14}/k_{15}$; $K_{17} = k_{16}/k_{17}$. wj are jth rates of the product formation, according to Scheme 1.

12. $Z''_0 + NA \xrightarrow{r_{12}} Z''_3$;
13. $Z''_3 + O_2 \xrightarrow{O_2,\, r_{13}} Z''_0 + H_2O + CO_2$;

Here Z''_0 – oxidized sites, Z''_1, Z''_2, Z''_3 – carbonate–carboxylate complexes of adsorbed NA, PA, βP, respectively.

3.3.3. *Formation of pyridine-3-nitrile from βP and NA (stages 14–17):*

14. $Z_N + \beta P \xrightarrow{r_{14}} Z_{1N}$;
15. $Z_{1N} + O_2 \xrightarrow{r_{15}} Z_N + PN + H_2O$;
16. $Z_N + NA \xrightarrow{r_{16}} Z_{2N}$;
17. $Z_{2N} + O_2 \xrightarrow{r_{17}} Z_N + PN + H_2O$

Here Z_N—active sites containing nitrogen, Z_{1N} and Z_{2N}—surface complexes of βP and NA, respectively.

Kinetic model of the reaction rates of the products formation corresponds to the scheme of stages 1–17. Kinetic rate equations of jth route (w_j) were derived by using the graph theory [63], and are listed in Table 2.

3.4. *Estimation of parameters of the kinetic model*

Parameters of the kinetic model were estimated by the procedure set forth below. A system of algebraic equations describing material balance in the test set-up was solved for each experimental point with fixed parameters of the kinetic model:

$$C_i^0 - C_i - W_i \times \frac{S_{CAT} \cdot G \cdot 3600}{V_f} = 0. \qquad (6)$$

Here C_i^0 and C_i are inlet and outlet concentrations of the ith reagent, respectively, mol m^{-3}; W_i is the accumulation rate of the ith reagent (Eqs. (1)–(5)) according to the given kinetic model, see rate equations in Table 2; G is the weight of catalyst sample, g; V_f is the flow rate, m^3 h^{-1}.

By solving Eq. (6), concentrations C_i were calculated for each individual run. The calculated values of concentrations were compared with the experimental values, and the vector of parameters of the kinetic model was estimated by minimization of the function $\varphi(K)$ defined as

$$\varphi = \min \frac{1}{N} \sum_{i=1}^{N} \sum_{j=1}^{5} |C_{i,j}^{exp} - C_{i,j}^{calc}|. \qquad (7)$$

Here j = 1, 2, 3, 4, 5 denote βP, NA, PA, CO_2 and PN, respectively; i is the number of the run; N is the total number of experimental points used in the minimization procedure.

For minimization of a sum of deviations of calculated values from experimental ones, a procedure based on Rosenbrock algorithm [64] was used.

Statistic characteristics of the estimates of kinetic model parameters were obtained according to the method described in [65]. After elimination of the outbreakers, 65 experimental points were retained. From this set, arbitrary 45 points were chosen, and parameters of kinetic model were estimated. This procedure was repeated several times for another set of 45 points. From the complete set of estimates mathematical expectation $\mu = (1/N)\sum_{i=1}^{N} K_i$ and dispersion $\sigma^2 = (1/N)\sum_{i=1}^{N}(K_i - \mu)^2$ were calculated.

As the dimension of system was too large (34 parameters to be estimated), the optimal parameters were determined step-by-step. First, a set of rate constants K_i was estimated for given temperatures. Then, a set of apparent energy activations E_i was estimated from Arrhenius law. Finally, a set of parameters evaluated at 270, 285 and 300 °C was corrected at a definite temperature with respect to functions $C(\tau)$.

Kinetic parameters, including rate constants Ki and activation energies E_i are listed in Table 2. All parameters are estimated for a catalyst particle of commercial size.

The correlation between the experimental and calculated values for conversion of β-picoline and for concentration of products is presented in Fig. 5. The average deviations

$$\Delta C = \frac{1}{N}\left[\sum \frac{(C_i^{calc} - C_i^{exp})^2}{(C_i^{calc})^2}\right]$$

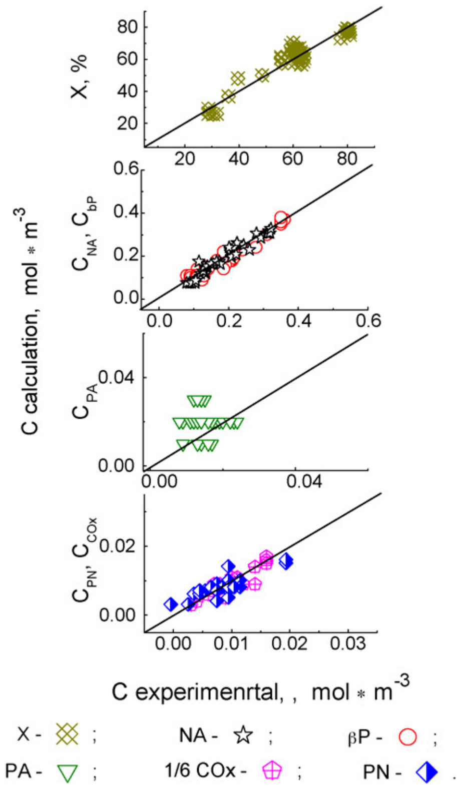

Fig. 5. Correlation between the calculated and the experimental values for β-picoline conversion and for concentrations of NA, PA, PN, 1/6CO_X and βP, mol m^{-3}.

of the calculated concentrations from the experimental ones lie within the experimental error limits: $\Delta C_{\beta P} = 2.2\%$, $\Delta C_{NA} = 1.6\%$, $\Delta C_{PA} = 7.5\%$, $\Delta C_{CO_2} = 3.4\%$, $\Delta C_{PN} = 1.3\%$; and for βP conversion $\Delta X = 2.7\%$ (Fig. 5).

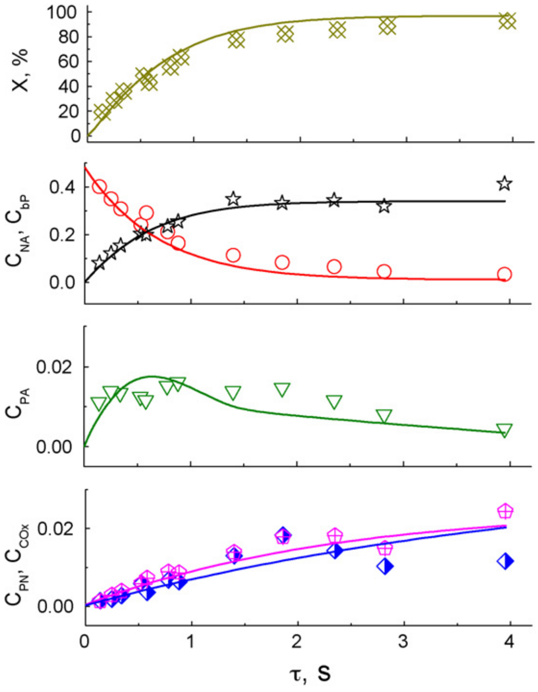

Fig. 6. Experimental and predicted data vs. contact time in differential reactor. Lines are calculated values, points are experimental values. Nomenclature of symbols see Fig. 5. $T = 270\,^{\circ}C$; inlet gas composition βP:O_2:H_2O = 1.08:21:20 (mol.%); τ = 0–3.95 s.

PA is an intermediate product, whose concentrations in the course of experimental runs do not exceed 0.008 vol.%. Error in its GC determination can be rather high. This is the reason of not-so-great correlation between the calculated and the experimental data on PA (Figs. 5 and 6).

Outlet concentrations of all reaction products were calculated on the base of the proposed kinetic model at the following conditions: temperature 270 °C; inlet composition βP:O_2:H_2O = 1.08:21:20 (mol.%); τ = 0– 3.95 s. The predicted and the experimental concentration profiles show good agreement (Fig. 6, and Figs. 2–4), thus kinetic model adequately describes the reaction behavior at given conditions.

4. Conclusions

Formation of nicotinic acid over V_2O_5-TiO_2 catalyst directly from βP and via intermediate product PA can be represented by a parallel-consecutive reaction scheme. It was found that β-picoline has an effect on the formation of nicotinic acid and methyl-3-carbaldehyde; oxygen affects the formation of nicotinic acid; water increases the rate of formation of NA and PA, but has no effect on their further oxidation to CO_X. Specific surface species and lattice oxygen of catalyst take part in the process of NA formation. Final product could be desorbed from the catalyst surface only if the oxygen is in gas phase.

Kinetic model of reactions was developed on the base of detailed kinetic studies and using *in situ* FTIR spectroscopy data. The model with optimal parameters shows satisfactory agreement between predicted and experimental data.

Acknowledgement

This work was performed under partial financial support from Russian Foundation for Basic Research (Grant no. 06-03-32473-a).

References

[1] B. Grzybowska, Catal. Today 1 (1987) 341–346.
[2] M.V. Shimanskaya, Ya.F. Oshis, L.Ya. Leytis, I.G. Iovel, Yu.Sh. Goldberg, L.O. Golender, A.A. Andersen, A.A. Avots, in: M.V. Shimanskaya (Ed.), Advances of Heterogeneous Catalysis in the Chemistry of Heterocyclic Compounds, Zinatne, Riga, 1984, 175 pp.
[3] P. Courtine, E. Bordes, Appl. Catal. A: Gen. 157 (1997) 45–65.
[4] A. Martin, Top. Catal. 29 (2004) 201–206.
[5] A. Martin, B. Lücke, Catal. Today 57 (2000) 61–70.
[6] D.A. Bulushev, L. Kiwi-Minsker, A. Renken, Catal. Today 57 (2000) 231–239.
[7] L. Kiwi-Minsker, D.A. Bulushev, F. Rainone, A. Renken, J. Mol. Catal. A 184 (2002) 223–235.
[8] H. Ge, G. Chen, Q. Yuan, H. Li, Chem. Eng. J. 127 (2007) 39–46.
[9] A.J. Hengstum, J. Pranger, S.M. Hengstum-Nuhuis, J.G. Ommen, P.J. Gellings, J. Catal. 101 (1986) 323–330.
[10] A. Martin, Y. Zhang, M. Meisel, React. Kinet. Catal. Lett. 60 (1997) 3–8.
[11] A.A. Yabrov, A.A. Ivanov, React. Kinet. Catal. Lett. 14 (1980) 347–352.
[12] C.R. Dias, M.F. Portela, G.C. Bond, J. Catal. 157 (1995) 344–352.
[13] C.R. Dias, M.F. Portela, G.C. Bond, J. Catal. 164 (1996) 276–287.
[14] J.N. Papageorgiou, G.F. Forment, Chem. Eng. Sci. 51 (1996) 2091–2098.
[15] A.I. Anastasov, Chem. Eng. Sci. 58 (2003) 89–98.
[16] M.P. Gimeno, J. Gason, C. Tellez, J. Herguido, M. Menendez, Chem. Eng. Process. 47 (2008) 1844–1852.
[17] B.V. Suvorov, Ammoxidation of Organic Compounds, Nauka, Alma–Ata, Russia, 1971.
[18] S.L.T. Andersson, S. Järås, J. Catal. 64 (1980) 51–67.
[19] A. Andersson, S.T. Lundin, J. Catal. 65 (1980) 9–15.
[20] B.V. Suvorov, N.A. Belova, V.I. Gostev, Kinet. Catal. 34 (1993) 296.
[21] A. Martin, B. Lucke, H. Seeboth, G. Ladwig, Appl. Catal. 49 (1989) 205–211.
[22] K.V. Narayana, A. Venugopal, K.S.R. Rao, V.V. Rao, S.K. Masthan, P.K. Rao, Appl. Catal. A 150 (1997) 269–278.
[23] A. Martin, V.N. Kalevaru, B. Lücke, A. Brükner, Appl. Catal. A 335 (2008) 196–203.
[24] V.N. Kalevaru, B.D. Raju, V.V. Rao, A. Martin, Appl. Catal. A 352 (2009) 223–233.
[25] E.M. Alkaeva, T.V. Andrushkevich, G.A. Zenkovets, M.G. Makarenko, WO Patent 9520577; Chem. Abstr. 129 (1996) 8632.
[26] E.M. Alkaeva, T.V. Andrushkevich, G.A. Zenkovetz, Proceedings of the 1st World Conference on Environmental Catalysis, Rome, Italy, 1995, p. 447.

[27] D. Heinz, W. Hoelderich, S. Krill, W. Boeck, K. Huthmacher: DE Patent 19, 839,559 A12000.03.02 (2000).
[28] D. Heinz, W.F. Hoelderich, S. Krill, W. Boech, K. Huthmacher, J. Catal. 192 (2000) 1–10.
[29] E.M. Alkaeva, T.V. Andrushkevich, G.A. Zenkovets, D.E. Babushkin, Catal. Lett. 54 (1998) 149–152.
[30] R. Chuck, Appl. Catal. A: Gen. 280 (2005) 75–82.
[31] SU, N 525425, 15.08.76, C 07 D 213/80.
[32] SU, N 235764, 24.01.69, C 07 D 213/80.
[33] J. Heveling, E. Armbruster, L. Utiger, M. Rohner, H.-R. Dettwiler, R.J. Chuck, EP 770,687 A 19,970. 502 (1997), to Lonza AG, Switzerland.
[34] H. Beschke, H. Friedrich, J. Heilos, DE 3,107,755 Al 1982.09.16 (1982), to Degussa-Huels AG, Fed. Rep. Ger.
[35] P.T. Anastas, J.B. Zimmerman, Sustainability Sci. Eng. 1 (2006) 11–32.
[36] W.A. Hoelderich, Catal. Today 62 (2000) 115–130.
[37] G.Ya. Popova, T.V. Andrushkevich, Yu.A. Chesalov, E.V. Ovchinnikova, React. Kinet. Catal. Lett. 87 (2006) 387–394.
[38] G.Ya. Popova, T.V. Andrushkevich, Yu.A. Chesalov, React. Kinet. Catal. Lett. 83 (2004) 353–360.
[39] Z. Song, T. Matsushita, T. Shishido, K. Takehira, J. Catal. 218 (2003) 32–41.
[40] T. Shishido, Z. Song, T. Matsushita, K. Takaki, K. Takehira, Phys. Chem. Chem. Phys. 5 (2003) 2710–2718.
[41] T. Shishido, Z. Song, T. Matsushita, E. Kadowaki, Y. Wang, K. Takehira, Appl. Catal. A 239 (2003) 287–296.
[42] Yu.A.Chesalov, G.Ya.Popova, T.V. Andrushkevich, React. Kinet. Catal. Lett., in press.
[43] E.V. Ovchinnikova, T.V. Andrushkevich, L.A. Shadrina, React. Kinet. Catal. Lett. 82 (2004) 191–197.
[44] V.V. Malakhov, I.G. Vasilyeva, Russ. Chem. Rev. 77 (2008) 350.
[45] V.M. Bondareva, T.V. Andrushkevich, O.B. Lapina, V.V. Malahov, L.S. Dovlitova, A.A. Vlasov, Kinet. Catal. 41 (2000) 736–744 (Russia).
[46] V.M. Bondareva, E.V. Ovchinnikova, T.V. Andrushkevich, React. Kinet. Catal. Lett. 94 (2008) 327–336.
[47] V.N. Kashkin, E.V. Ovchinnikova, A.P. Kagyrmanova, V.N. Bibin, G.Ya. Popova, I.A. Zolotarsky, G.A. Zenkovetz, T.V. Andrushkevich: Abstracts, CHEMREACTOR-17, Athens-Crete, Greece, May 15–19 (2006).
[48] S. Anniballi, F. Cavani, A. Guerrini, B. Panzacchi, F. Trifiro, C. Fumagalli, R. Leanza, G. Mazzonni, Catal. Today 78 (2003) 117–129.
[49] B. Delmon, Stud. Surf. Sci. Catal. 110 (1995) 43.
[50] J.C. Vedrine, J.M.M. Millet, J.-C. Volta, Catal. Today 32 (2000)115.
[51] J. Barrault, C. Batiot, L. Magaud, M. Ganne, Stud. Surf. Sci. Catal. 110 (1997)375.
[52] E.M. Erenburg, T.V. Andrushkevich, W.N. Bibin, Kinet. Catal. 20 (1979) 680.
[53] M. Ai, Catal. Today 42 (1998) 297.
[54] Ch.-H. Zin, H. Bai, Appl. Catal. B 42 (2003) 279.
[55] V.M. Bondareva, T.V. Andrushkevich, Yu.D. Pankratiev, React. Kinet. Catal. Lett. 61 (1997) 337.
[56] E.V. Ovchinnikova, Yu.A. Chesalov, G.Ya. Popova, T.V. Andrushkevich, 6th World Congress on Oxidation Catalysis, 2009 (Abstracts).
[57] G.Ya. Popova, T.V. Andrushkevich, Yu.A. Chesalov, V.N. Parmon, J. Mol. Catal. A 268 (2007) 251–256.
[58] A.A. Davydov, in: N.T. Sheppard (Ed.), Molecular Spectroscopy of Oxide Catalyst Surfaces, J. Wiley, Chichester, 2003.
[59] T.V. Andrushkevich, Kinet. Catal. 38 (1997) 266–276.
[60] G.Ya. Popova, A.A. Davydov, T.V. Andrushkevich, I.I. Zakharov, Kinet. Catal. 36 (1995) 125–136.
[61] G.K. Boreskov, in: K.I. Zamaraev, A.V. Khasin (Eds.), Heterogeneous Catalysis, Nova Science Publishers, Hauppauge, 2003.
[62] E.V. Ovchinnikova, T.V. Andrushkevich, React. Kinet. Catal. Lett. 93 (2008) 203–210.
[63] G.S. Yablonskii, V.I. Bykov, A.N. Gorban, V.I. Elokhin, Comprehensive Chemical Kinetics in: R.G. Compton (Ed.), Kinetic Models of Catalytic Reactions, vol. 32, Elsevier, Amsterdam/Oxford/New York/Tokyo, 1991 (Chapter 4).
[64] H.H. Rosenbrock, C. Storey, Computational Techniques for Chemical Engineers, Pergamon Press, New York, 1968, p. 107.
[65] D.M. Himmelblau, Process Analysis by Statistical Methods, 1970.